

Extended X-ray emission around 4C 41.17 at $z = 3.8$

Caleb Scharf

*Columbia Astrophysics Laboratory, Columbia University, MC5247, 550 West 120th St.,
New York, NY 10027, USA.*

caleb@astro.columbia.edu

Ian Smail

Institute for Computational Cosmology, University of Durham, South Rd, Durham UK

ian.smail@durham.ac.uk

Rob Ivison

Astronomy Technology Centre, Royal Observatory Edinburgh, Blackford Hill, Edinburgh UK

rji@roe.ac.uk

Richard Bower

Institute for Computational Cosmology, University of Durham, South Rd, Durham UK

r.g.bower@durham.ac.uk

Wil van Breugel

University of California, Lawrence Livermore National Laboratory, Livermore, CA, USA

wil@igpp.ucllnl.org

Michiel Reuland

Leiden Observatory, Leiden 2300 RA, The Netherlands

mreuland@igpp.ucllnl.org

ABSTRACT

We present sensitive, high-resolution, X-ray imaging from *Chandra* of the high-redshift radio galaxy 4C 41.17 ($z = 3.8$). Our 150-ks *Chandra* exposure detects strong X-ray emission from a point source coincident with the nucleus of the

radio galaxy. In addition we identify extended X-ray emission with a luminosity $\sim 10^{45}$ erg s $^{-1}$ covering a 100 kpc (15'') diameter region around the radio galaxy. The extended X-ray emission follows the general distribution of radio emission in the radio lobes of this source, and the distribution of a giant Lyman- α emission line halo, while the spectrum of the X-ray emission is non-thermal and has a power law index consistent with that of the radio synchrotron. We conclude that the X-ray emission is most likely Inverse-Compton scattering of far-infrared photons from a relativistic electron population probably associated with past and current activity from the central object. Assuming an equipartition magnetic field the CMB energy density at $z = 3.8$ can only account for at most 40% of the Inverse-Compton emission. Published submillimeter maps of 4C 41.17 have detected an apparently extended and extremely luminous far-infrared emission around the radio galaxy. We demonstrate that this photon component and its spatial distribution, in combination with the CMB can reproduce the observed X-ray luminosity. We propose that photo-ionization by these Inverse-Compton X-ray photons plays a significant role in this system, and provides a new physical feedback mechanism to preferentially affect the gas within the most massive halos at high redshift. This is the highest redshift example of extended X-ray emission around a radio galaxy currently known and points towards an extraordinary halo around such systems, where cool dust, relativistic electrons, neutral and ionized gas, and intense infrared and X-ray radiation all appear to coexist.

Subject headings: galaxies: active – galaxies: X-ray – galaxies: jets – galaxies: radio galaxies individual: 4C 41.17 – radiation mechanisms: non thermal

1. Introduction

One of the major results from *Chandra* observations of low and intermediate redshift galaxy clusters is the identification of bubble-like structures in the X-ray images (McNamara et al. 2000). This phenomenon was first seen with *ROSAT* in the Perseus and Cygnus-A clusters (Boehringer et al. 1993; Carilli, Perley, & Harris 1994). These cavities are apparently associated with energy injection due to nuclear activity from active galactic nuclei (AGN) in the brightest cluster galaxies. It appears that powerful radio jets are particularly effective mechanisms for inputting mechanical energy to the intracluster medium (ICM). This activity may influence the structure and energetics of gas in the highest density regions in the clusters. The redistribution of gas produced by this injection of energy may have particularly profound consequences for the rate of cooling of gas in these regions. This would have an impact on a

variety of fields, including theoretical modeling of galaxy formation – as large-scale cooling of gas is a critical route for building the baryonic mass of galaxies (Cole et al. 2000). Studying the influence of AGN on their surroundings is therefore important for determining the capacity of this form of feed-back to delay the on-set of gas accretion and star-formation in massive galaxies at high redshifts. The scaling properties of the ICM are also best explained by an absence of large amounts of very low entropy gas in cluster cores (Kaiser 1991; Evrard & Henry 1991; Mushotzky & Scharf 1997). Finding a workable mechanism for accomplishing this is at the forefront of cluster formation studies, e.g. Tozzi & Norman (2001a); Voit et al. (2002), and likely candidates are heating and cooling of the ICM.

Investigating the possibility that radio sources influence the thermodynamics of dense gas in their environments is further motivated by observations which demonstrate that individual, luminous, radio galaxies at high redshifts ($z > 2$) reside in apparently overdense regions: as traced through excesses of Lyman-break galaxies, Lyman- α emitters, Extremely Red Objects, X-ray detected AGN or luminous submillimeter galaxies (Pentericci et al. 2000; Kurk et al. 2000; Chapman, McCarthy & Persson 2000; Pentericci et al. 2002; Ivison et al. 2000). Thus the feedback from AGN (and star formation) in bright radio sources may have had ample opportunity to influence the formation and evolution of galaxies in regions which are believed to evolve into the cores of clusters at the present-day. Studying luminous radio galaxies in high-density environments at high redshifts therefore provides an important route to track the changing effects of feedback during the formation of a massive cluster of galaxies.

Early studies of the X-ray environments of powerful radio galaxies were limited by the modest spatial resolution of the X-ray observations (Brunetti 2002). However, with arcsecond resolution, high sensitivity and good spectral resolution from *Chandra* there have been two published searches for hot gas in the vicinity of radio galaxies and radio-loud quasars at $z > 1$ (Fabian et al. 2001, 2003a; Carilli et al. 1998, 2002). One study detects extended emission at $z = 1.79$ with a mildly favored non-thermal origin and a remarkable morphology (3C 294, Fabian et al. (2003a)) and the other, with a detection of extended emission at $z = 2.16$, has been argued to be thermal in origin, although the data is somewhat lower signal-to-noise (PKS 1138-262, Carilli et al. (1998, 2002)).

In this paper we present a deep *Chandra* observation of one of the most distant and powerful high-redshift radio galaxies; 4C 41.17 at $z = 3.8$. Recent submillimeter observations of this galaxy using the SCUBA camera have detected intense, and apparently spatially-resolved, submm emission from the radio galaxy (Ivison et al. 2000; Stevens et al. 2003). This emission is thermal radiation coming from dust grains within the galaxy which are heated by UV photons from young stars or an AGN (e.g. Smail et al. (2002)). The far-

infrared luminosity of the galaxy is in excess of $10^{13} L_{\odot}$ and the inferred mass of dust is around $6 \times 10^8 M_{\odot}$ (Stevens et al. 2003), both of which suggest intense star formation is occurring within 4C 41.17. Further evidence for extreme activity occurring in the vicinity of the radio galaxy includes the presence of an extended Lyman- α halo reaching to >100 kpc (Chambers, Miley, & van Breugel (1990); Dey et al. (1997); Reuland et al. (2003); Figure 5) as well as spatially-extended [OII] and [OIII] emission on similar scales (van Breugel et al. 2002). Dey et al. (1997) have also shown from spectropolarimetric observations that the dominant contribution to the restframe UV emission in 4C 41.17 must be due to young stars, with a formation rate of $140\text{--}1100 h_{50}^{-2} M_{\odot}$, possibly triggered by the expansion of the radio source (see also van Breugel et al. (1999)).

Strong evidence exists for the immediate environment of 4C 41.17 being overdense and consistent with a “proto-cluster” region. In particular, in parallel to detecting the resolved submm emission from the radio galaxy, Ivison et al. (2000) also tentatively identified an overdensity of bright SCUBA galaxies in a 1-Mpc region around the radio source. They interpreted this as evidence for vigorous dust-obscured star formation and AGN activity during the formation of other massive galaxies clustered around the radio galaxy. In addition to this highly obscured, massive galaxy population, Lacy & Rawlings (1996) have suggested that there is a modest excess of Lyman-break galaxies in this region, having found six candidate $z \sim 3.8$ galaxies in a 1.5-arcmin^2 field, roughly centered on 4C 41.17. They show that this density is slightly higher than that expected in blank fields, although this comparison is uncertain, and issues of cosmic variance also make it difficult to assess this over-density (Steidel et al. 1999). We also note that spectroscopy of candidate Lyman- α emission line objects in this field has so far confirmed three sources at the redshift of the radio galaxy in a 3.5-arcmin^2 field, showing an apparent over-density of Lyman- α emitters in this field (van Breugel et al. 2002).

Throughout this work we assume a cosmology with $H_0 = 70 \text{ km s}^{-1} \text{ Mpc}^{-1}$, $\Omega_0 = 0.3$, and $\lambda_0 = 0.7$, consistent with the WMAP parameters (Spergel et al. 2003). In this cosmology at $z = 3.8$, $1''$ corresponds to 7.1 kpc, the Universe is 1.6 Gyrs old and the lookback time is 88% of the age of the Universe.

2. *Chandra* Data Analysis

The *Chandra* observation of 4C 41.17 was made during Sept 25–26 2002. 150 ks of exposure was obtained using the back-illuminated S3 chip in VFaint mode with two consecutive exposures of ~ 75 ksec. After good-time filtering, 135 ksec of usable exposure remained. The data were re-processed using the standard CIAO tools to exploit the additional background

discrimination of the VFAINT mode telemetry. A processed image of 4C 41.17 is presented in Figure 1. Appropriate RMF’s and ARF’s were generated for the primary 4C 41.17 source location on the S3 chip. Since the S3 chip is currently CTI-uncalibrated no CTI correction was made to the data.

This observation detects two components of emission associated with 4C 41.17. The first of these is a bright point-source at 06 50 52.07 +41 30 31.17 (J2000)¹. This X-ray source lies within 0.5’’ of the position of the radio core (which itself lies $\sim 0.5''$ east of B1 in Figure 2, (Bicknell et al. 2000)) and hence is positionally coincident with this component to the limit of our astrometric precision.

The second X-ray component is a region of diffuse emission surrounding this point source (Figures 1, 2 & 3). This emission drops away as $\sim 1/r^2$ to the North-East, but is significantly more extended along the direction of the radio jet to the South-West. To measure fluxes for the point-source and extended components we define an aperture for the point source as a 1’’ square region which fully encompasses the 90% flux-enclosed PSF at the on-axis S3 position. In contrast, fluxes for the diffuse component were measured using an elliptical aperture orientated along the major axis of the 4C 41.17 emission (see Figure 3). Background regions were accumulated from (a) 10 blank sky regions in this S3 data, selected to be close to the aimpoint and therefore less subject to chip-wide variations, and totaling approximately 4 arcmin² (b) blank sky regions from the available blank-sky files. The effect of utilizing (a) versus (b) in the following analyses was negligible given our other uncertainties.

Total count rates were measured for both components in the 0.3–10 keV bandpass (restframe 1.44–48 keV). For the diffuse component of 4C 41.17 a total count of 200 photons was obtained. The estimated background from the unresolved X-ray background (XRB) was 75 ± 10 counts, with an effective exposure time of 135.113 ks, yielding a background subtracted count rate of $9.3 \pm 0.9 \times 10^{-4}$ ct s⁻¹ (see below for estimated luminosities). For the point source, 51 photons were measured in the 1’’ \times 1’’ aperture. By interpolating the surrounding diffuse component we have estimated a maximum contribution to the point emission of 14 ± 4 photons, the contribution of the unresolved XRB is negligible for this small region. The background subtracted point source emission therefore has a count rate $2.7 \pm 0.8 \times 10^{-4}$ ct s⁻¹.

Owing to its smaller photon count we restrict our spectral analysis of the point source

¹This position is accurate to $\pm 0.5''$ and has been corrected to the radio coordinate frame using the position of a hard X-ray source 40’’ south of 4C 41.17 which is well detected at 1.4 GHz, the offset between the nominal X-ray and radio coordinates for this source was: -0.042 s, $-0.09''$.

to simply evaluating its hardness ratio (defined as $(H - S)/(H + S)$ with the energy ranges of the soft band (S) of 0.5–2 keV and for the hard band (H) 2–10 keV, both in the observed frame). We estimate a hardness ratio of 0.00 ± 0.55 and based on previous surveys we conclude that this is consistent with the expected characteristics of a high- z Type II AGN (Rosati et al. 2002; Tozzi et al. 2001b), although Type I (with hardness ratios ~ -0.5) cannot be ruled out. In estimating the intrinsic luminosity we have therefore adopted the mean photon index $\Gamma = 1.5$, ($N(E) \propto E^{-\Gamma}$), and large intrinsic absorption, $n(\text{HI}) \simeq 10^{23} \text{ cm}^{-2}$ determined by Tozzi et al. (2001b) for $z > 1$ Type-II sources with similar hardness ratios. Changing these properties by 10–20% (and ignoring absorption) has negligible impact on our results. We determine a flux for the point source (unabsorbed by Galactic $n(\text{HI})$) of $3.4 \pm 1.0 \times 10^{-15} \text{ erg s}^{-1} \text{ cm}^{-2}$ (0.3-10 keV) and a luminosity of $8.8 \pm 2.5 \times 10^{43} \text{ erg s}^{-1}$ (0.3-10 keV rest frame), or $4.6 \pm 1.3 \times 10^{44} \text{ erg s}^{-1}$ (1.44-48 keV rest frame, corresponding to the 0.3-10 keV observed band and therefore the least extrapolation).

There are sufficient photons detected in the extended component for us to attempt a slightly more sophisticated analysis. We begin by constructing a 20 ct per bin, 10 bin spectrum on which conventional spectral analysis can be performed. We find that this spectrum is inconsistent with thermal bremsstrahlung but an excellent fit is obtained with a single index power law (using XSPEC & background subtraction). The best fit photon index (0.3 – 7 keV) was $\Gamma = 1.29 \pm 0.18$ (90% confidence limits) with $n(\text{HI})$ fixed at the Galactic value of $1 \times 10^{21} \text{ cm}^{-2}$ (see Figure 4), and reduced $\chi^2 = 1.3$. For comparison, the measured hardness ratio is -0.21 ± 0.31 , also consistent with a hard spectrum. No satisfactory fit could be obtained with a thermal MEKAL model, kT was constrained as $> 97 \text{ keV}$ in the restframe at $z = 3.8$. This is not surprising since even a 10 keV Raymond-Smith spectrum exhibits relatively little photon count above 4 keV, corresponding to an observed energy (given $z = 3.8$) of 0.83 keV, while we clearly detect the bulk of flux at higher energies (Figure 4).

Fitting an intrinsically absorbed power law (at $z = 3.8$) gave a best fit of $\Gamma = 1.6 \pm 0.3$ and $n(\text{HI}) = 3 \pm 3 \times 10^{22} \text{ cm}^{-2}$. We do not consider this model further as it is difficult to credit such strong absorption being distributed over such a large volume. A comparison of the extended X-ray emission to the North-east and South-west of the point source shows no significant difference in the spectral properties of these two regions (see Figure 2).

We also test the spectrum using the preliminary ACISABS model designed to model the modified ACIS soft response due to molecular contamination and fitting for energies 0.4 – 7 keV (Chartas & Getman 2002). With $n(\text{HI})$ fixed at the Galactic value we obtain a best fit power law of $\Gamma = 1.57 \pm 0.26$ (90%) and reduced $\chi^2 = 0.7$. A thermal spectrum fit with the ACISABS response yields a best fit of $42 \pm 42 \text{ keV}$ (reduced $\chi^2 = 0.86$).

Using our total count rate for the diffuse emission associated with 4C 41.17 and assuming the measured photon index of $\Gamma = 1.57 \pm 0.26$ obtained with the ACISABS response and the Galactic $n(\text{HI})$ column density we estimate an unabsorbed flux of $1.14_{-0.11}^{+0.16} (\pm 0.11) \times 10^{-14} \text{ erg s cm}^{-2}$ (0.3-10 keV). The errors correspond to the uncertainty in the photon index and the Poisson uncertainty in photon counts respectively and are presented in this form to allow for the systematic nature of the error propagated from the power law index.

For our adopted cosmology we therefore estimate an X-ray luminosity of $L_X = 1.5_{-0.3}^{+0.4} (\pm 0.2) \times 10^{45} \text{ erg s}^{-1}$ (1.44-48 keV rest frame, corresponding to the 0.3-10 keV observed frame) or $L_X = 7.5_{-1.5}^{+2.1} (\pm 0.8) \times 10^{44} \text{ erg s}^{-1}$ (0.3-10 keV rest frame).

We have performed several tests to evaluate the limits on a possible thermal component in the diffuse emission around 4C 41.17. As described above, an unsatisfactory fit to a thermal spectrum (MEKAL model) was obtained for the full spectrum. Subdividing the spectrum between 0.3–2 keV (1.44–9.6 keV rest frame) and 2–10 keV (9.6-48 keV rest frame), each with 5 spectral bins, also yielded best power-law fits, consistent to within 90% errors with each other and with the $\Gamma = 1.29$ or $\Gamma = 1.57$ (ACISABS applied) overall fit and normalization. Fitting a joint thermal and power law spectrum to the full dataset again resulted in an essentially unconstrained thermal component. Finally, we fit a power law to the > 1 keV data, fixed Γ to the best slope (1.6 ± 0.4) and then fit for the spectral normalization at < 1 keV. Again, the best-fit normalization was entirely consistent between these two bands. Very conservatively, the upper limit to any thermal emission must therefore be equal to, or less than, the Poisson fluctuation in photon counts in the band 0.3–0.83 (i.e. rest frame 1.4–4 keV, assuming negligible thermal emission from > 4 keV). This yields a count rate limit of $< 4 \times 10^{-5} \text{ ct s}^{-1}$ (0.3–0.83 keV) or an unabsorbed bolometric flux (assuming a generic 4 keV plasma) of $\leq 3 \times 10^{-16} \text{ erg s}^{-1} \text{ cm}^{-2}$. This corresponds to a bolometric luminosity limit for a thermal spectrum of $L_X \leq 4.1 \times 10^{43} \text{ erg s}^{-1}$ (i.e. $\leq 3\%$ of the 1.44-48 keV rest frame luminosity). Thus, while we can only rule out the presence of an X-ray emitting cluster with a luminosity some 40% of that of the Virgo cluster, it is clear that the dominant source of the extended X-ray emission is non-thermal.

In summary: the unresolved X-ray source within 4C 41.17 has a luminosity and spectral properties consistent with a heavily obscured, luminous AGN (Type-II). While the diffuse X-ray component around 4C 41.17 is most likely non-thermal in origin, with a power-law spectrum and significant luminosity. We limit the contribution from any thermal component to less than $\sim 4 \times 10^{43} \text{ erg s}^{-1}$.

3. The nature of the diffuse X-ray emission around 4C 41.17

In addition to 4C 41.17, extended X-ray emission has been detected around a number of moderate and high-redshift radio galaxies and radio-loud quasars and these exhibit a variety of strength of correlation between the morphologies in the X-ray and radio bands (Crawford et al. 1999; Chartas et al. 2000; Schwartz et al. 2000; Celotti, Ghisellini, & Chiaberge 2001; Siemiginowska et al. 2002; Brunetti et al. 2001; Worrall et al. 2001; Carilli et al. 2002; Fabian et al. 2003a; Fabian, Celotti, & Johnstone 2003b; Donahue, Daly & Horner 2003; Comastri et al. 2003). However, the precise origin of the X-ray emission is still a matter of debate (Harris & Krawczynski 2002). Where there is a strong spatial correlation between the emission in the radio and X-ray bands the preferred mechanism could either be synchrotron emission or Inverse-Compton (IC) scattering by the relativistic electrons in the jet plasma of photons from the source itself or the Cosmic Microwave Background (CMB). Where there is less apparent spatial correlation between the two wavebands (possibly due to weaker detections), there is more ambiguity. In some cases it has been suggested that the X-ray emission may be thermal in origin and arise from hot gas in a group or cluster-like structure (Carilli et al. 2002). In the case of 3C 294 (Fabian et al. 2003a), the X-ray emission is very clearly much more extended than the radio structure and exhibits remarkably sharp edge features. Fabian et al. (2003a) suggest that this is consistent with IC emission from an older population of relativistic electrons generated by previous episodes of nuclear activity and with confinement by a hot, unseen, ICM.

Further, tentative support for an IC mechanism operating in some high-redshift radio galaxies studied in the X-ray and radio bands comes from the apparent evolution of the L_X/L_R ratios. IC scattering from the CMB implies that the ratio of X-ray to radio luminosities should scale as $(1+z)^4$ (see Equation 1 below). Using published X-ray luminosities (see references above) and radio powers (Herbig & Readhead 1992) we find $L_X/L_R = 0.70$ (4C 41.17, $z = 3.798$), 0.21 (PKS 1138–262, $z = 2.156$), 0.11 (3C 9, $z = 2.012$), and 0.08 (3C 219, $z = 0.174$). These ratios are clearly subject to large uncertainties, such as the modeling of the X-ray emission, magnetic fields, and the presence of local far-infrared (FIR) photon sources. However, a general trend for increasing L_X/L_R with redshift appears to be present, although a poor fit to the expected $(1+z)^4$ scaling.

In the case of 4C 41.17, several pieces of evidence also point to a non-thermal IC origin of the diffuse emission. First, the restframe surface brightness of the emission is $(1+z)^4 I_x \sim 10^{-11} \text{ erg s}^{-1} \text{ cm}^{-2} \text{ arcmin}^{-2}$. This is a factor ~ 100 higher than ICM thermal emission in the brightest local galaxy clusters. IC scattering of CMB photons on the other hand has almost no redshift dependence owing to the cancellation of surface brightness dimming by the corresponding increase in energy density of the CMB with redshift (although variations

in magnetic field strength come into play).

Second, the measured spectrum of the X-ray emission is a power law, with an energy spectral index $\alpha \equiv 1 - \Gamma = -0.57 \pm 0.26$. As discussed by Chambers, Miley, & van Breugel (1990) the integrated radio spectrum of 4C 41.17 has a low frequency index of $\alpha \simeq -0.83$ (≤ 200 MHz rest frame), where synchrotron losses have a longer timescale, and an index of $\alpha \simeq -1.33$ for higher frequencies (200MHz-48GHz rest frame). If the X-ray emission is IC scattering then a large fraction of the flux must arise from electrons with synchrotron frequencies < 200 MHz (see Equation 2 below) and should exhibit the same spectral slope (Felten & Morrison 1966). Given the uncertainties in both the X-ray and radio spectral fits it appears that the energy spectral indices are indeed consistent – as would be expected if the X-ray and radio photons originated from the same particle population.

Thirdly, the overall morphology of the X-ray emission is indeed correlated with the radio maps (Figure 2), especially if one notes that the observed radio emission is at ~ 7.5 GHz rest frame. Since the radio spectrum is steep in this range ($\alpha \sim -1.3$) only the highest surface brightness features are seen in the maps. Moreover, since the radio source spectra steepen away from the hotspot towards the AGN, the radio morphology at low frequencies is somewhat different from that at higher frequencies, with relatively bright ‘bridges’ and fainter hotspots (e.g. Cygnus-A). A large abundance of low energy electrons in the bridges would result in increased IC losses and thus brighter X-ray emission from these structures as compared to the hotspots (modulo the photon field distribution, see below). The primary electron population for IC scattering of the CMB photons must have $\gamma \sim 1000$, or if we are seeing IC scattering of local FIR photons then the electrons will have $\gamma \sim 100$. By contrast, the electrons responsible for the bulk of the observed radio synchrotron emission (5-25 GHz rest frame) have $\gamma \sim 5000$ (Brunetti 2002). The general, but not point-by-point, correlation of radio and X-ray emission (Figures 2 & 5) is therefore not unexpected and offers clues to the electron distribution and AGN activity. We discuss this in more detail below.

Finally, although our X-ray data are currently too noisy for a definitive measurement, the surface brightness distribution appears to be relatively flat but with quite well delineated edges (e.g. Figure 1). As discussed by Fabian et al. (2003a) for the case of 3C 294, this suggests confinement of an electron population by an external, hot, medium – such as that already posited for 4C 41.17 (Carilli, Owen, & Harris (1994) and see §4).

While other, non-IC, non-thermal sources of X-ray emission cannot be entirely ruled out, all such sources will be dimmed by $(1 + z)^4$, a factor of 530 at $z = 3.8$, putting serious constraints on possible emission mechanisms. We suggest therefore that the most likely source for the diffuse X-ray emission around 4C 41.17 is IC scattering of CMB/FIR photons. We now discuss this mechanism in more detail, as well as the probable origin of the photons:

either the CMB alone or with a contribution from the known luminous FIR source.

The relative luminosity of the radio synchrotron and IC X-ray emission from scattering off a photon field is given by:

$$\frac{L_R}{L_X} = \frac{B^2/8\pi}{\rho} \quad , \quad (1)$$

where B is the magnetic field strength in the plasma and ρ is the energy density of the scattering photons. For the CMB, at a redshift z , $\rho_{CMB} = 7.56 \times 10^{-15} T_0^4 (1+z)^4 \text{ erg cm}^{-3}$ (Jones 1965; Felten & Morrison 1966; Schwartz 2002a,b). At $z = 3.8$ with $T_0 = 2.728\text{K}$ (Fixsen et al. 1996) $\rho_{CMB} = 2.2 \times 10^{-10} \text{ erg cm}^{-3}$.

The relationship between IC scattered energies, E , and the synchrotron frequencies emitted by electrons of a given energy is:

$$\langle E \rangle (eV) \approx 0.9 \times 10^2 \frac{T}{B(\mu G)} \nu_s (MHz) \quad , \quad (2)$$

where T is the characteristic photon temperature and ν_s is the synchrotron radio frequency (Felten & Morrison 1966).

The radio luminosity of 4C 41.17 integrated over all components is $L_R = 1.28 \times 10^{46} \text{ erg s}^{-1}$ (from Chambers, Miley, & van Breugel (1990) and converted to our adopted cosmology). In the following calculations we adopt a constant spectral index from 10-10,000 MHz of $\alpha = -1.33$ ($S_\nu = k\nu^\alpha$). This is conservative in the sense that it will slightly over-predict the low frequency luminosity and therefore slightly over-predict the expected IC X-ray emission. In Figure 5 we plot the IC X-ray luminosity predicted from the known radio spectrum of 4C 41.17 and Equations 1 and 2 (in a 1.44-48 keV rest frame energy band corresponding to the observed 0.3-10 counts and therefore requiring minimal extrapolation). The predicted L_x is shown for both CMB photons alone and for 3 cases in which the local mean FIR energy density over the emitting volume is 1, 2, and 3 times the CMB energy density.

Carilli, Owen, & Harris (1994) determine an equipartition field of $B = 50\text{--}80\mu\text{G}$ (their Appendix A, adjusted to our assumed cosmology) in the low surface brightness regions away from the radio hotspots. Figure 5 demonstrates that a significant contribution from the local FIR photons is necessary to produce the observed L_x if the equipartition B field is correct.

As discussed in §1, 4C 41.17 is one of the most luminous sub-mm sources known. The galaxy is detected at both $450\mu\text{m}$ and $850\mu\text{m}$ with fluxes of 35.3 mJy and 11.0 mJy respectively Ivison et al. (2000), implying a graybody temperature of $47 \pm 10 \text{ K}$ and

$L_{FIR} = 3.2_{-1.7}^{+3.2} \times 10^{13} L_{\odot}$ ($1.22_{-0.65}^{+1.22} \times 10^{47}$ ergs $^{-1}$) for our assumed cosmology. We note that this exceeds the integrated radio-synchrotron luminosity by a factor ~ 15 , showing that the sub-mm emission arises in a separate component of dust-reprocessed radiation from vigorous star formation or an AGN (Ivison et al. 2000).

If the local FIR emission is point-like and isotropic then the energy density at a distance R from the source is $\rho_{FIR} = 3L/4\pi cR^2$. For the observed L_{FIR} then the local photon energy density would exceed that of the CMB, $\rho_{FIR} > \rho_{CMB}$, out to a distance of 13 kpc from the source. Clearly then the local FIR photons can play a significant role in the observed IC emission and may provide the necessary boost in L_x required by Figure 5.

There is also evidence that the FIR source in 4C 41.17 is spatially extended. Ivison et al. (2000) claim that the thermal dust emission from 4C 41.17 is partially resolved on a scale of 50 kpc ($7''$, FWHM), after correcting for the SCUBA beam (Figure 2; see also Stevens et al. (2003)). This implies a physical extent of the submm emitting region of ~ 50 kpc. We adopt a very crude model for the dust cloud of a sphere of uniform emissivity and diameter D_{cloud} , this yields a mean FIR energy density of $\simeq 9L_{FIR}/2\pi cD_{cloud}^2$ within its volume. In this case the mean local FIR energy density in the cloud exceeds that of the CMB if D_{cloud} is *smaller* than 53_{-17}^{+22} kpc (errors from uncertainties in L_{FIR}). A slightly more realistic model has the relativistic plasma modeled as a cylindrical volume of length ~ 100 kpc, embedded in the cloud, this would then require that D_{cloud} must be *smaller* than ~ 60 kpc for the volume averaged energy density to be equal to or greater than that of the CMB over the entire emitting region, $\rho_{FIR} \geq \rho_{CMB}$.

Since this is comparable to the claimed size of the dust emission in this system from Ivison et al. (2000) it indicates that local FIR emission could plausibly make up the apparent shortfall in photons seen in Figure 5, although these estimates are subject to significant uncertainties and are designed to be illustrative rather than definitive. We note that the relatively flat X-ray emission profile in 4C 41.17 also suggests that the dominant source of local FIR photons arises in an extended component. However, the tentative evidence on the North-Eastern side for a $\sim 1/r^2$ drop-off (§2) suggests that the local FIR emission in that direction could have a more compact configuration.

We conclude that it appears necessary and likely inevitable that local FIR photons play a role in the IC X-ray emission (Figure 5). However, the inherent difficulties in constraining magnetic field strengths and the unknown true distribution of the electron population make more detailed estimates very difficult.

4. 4C 41.17: a forming massive galaxy in a proto-cluster

Early indications of the presence of a high-density gas environment around 4C 41.17 came from the detection of a strong and spatially variable rotation measure in polarimetry mapping of the various radio structures in the source (Carilli, Owen, & Harris 1994). These rotation measures indicate the presence of large column densities of magnetized, hot gas. Carilli, Owen, & Harris (1994) estimate a total gas mass of $\geq 10^{11} M_{\odot}$ (in our cosmology) and suggest that this material arises from an X-ray type “cooling flow” in a dense cluster environment around 4C 41.17. The results presented here do not rule out this scenario. Our limit of $\sim 4 \times 10^{43} \text{ erg s}^{-1}$ on thermal emission is still compatible with a much more spatially extended thermal component which may be accreting into the central potential and which would be surface brightness dimmed by $1/(1+z)^4$.

In an effort to further understand the distribution of matter in 4C 41.17 we make use here of a very deep Lyman- α image produced with a custom-built, high throughput interference filter with a 65 \AA bandpass centered at the redshifted Lyman- α line at 5839 \AA (for $z = 3.798$) with the Echellette Spectrograph and Imager (Sheinis et al. 2000) at the Cassegrain focus of the Keck II 10m telescope (these data have been previously discussed in van Breugel et al. (2002) and Reuland et al. (2003)). The data were obtained during photometric conditions and good seeing (FWHM = $0.57''$). With a total exposure time of 27.6 ks this Lyman- α image is the most sensitive obtained to date and reaches a surface brightness of $8.0 \times 10^{-19} \text{ erg s}^{-1} \text{ cm}^{-2} \text{ arcsec}^{-2}$ (3σ limit in a $2.0''$ diameter aperture). A broad-band R image, obtained as part of a multi-band spectral energy distribution study of the 4C 41.17 field (Reuland et al. 2003) was scaled and subtracted from the Lyman- α image to construct the pure emission-line image shown in Figure 6. In addition, extended [OII] $\lambda 3727$ and [OIII] $\lambda 5007$ emission has been detected, confirming that the Lyman- α arises from an ionized medium and not from scattering off a neutral gas. With a linear dimension of $\sim 150 \text{ kpc}$ at the detection limit, the 4C 41.17 nebula is the largest presently known (Reuland et al. 2003).

The Lyman- α halo shows distinct correlation features with the X-ray and radio maps, including several spur-like Lyman- α features, which also appear on slightly larger scales in the X-ray emission. The IC X-ray model as described in §3 might suggest that the X-ray emission would tend to be anti-correlated with Lyman- α emitting regions owing to the propensity of radio jets to evacuate gas from their volume. Indeed this would appear to match reasonably well the situation seen around the South-Western jet, A, in Figure 6. The Lyman- α spurs to the North and East are then anomalous, unless we consider an additional mechanism for producing a population of relativistic electrons correlated with the ionized Lyman- α gas.

The halo of a massive proto-galaxy is likely to consist of a multiphase medium of cool, $\leq 10^4$ K, clouds or filaments embedded in a virialized medium at 10^6 – 10^7 K (Rees 1989). In such a multi-phase medium the passage of a bow shock driven by an expanding radio source, or by starburst activity, may stimulate a range of behaviour. The densest patches are likely to be relatively unaffected by the passage of the shock, although they may collapse due to the increased pressure of the gas surrounding them. In contrast, the intermediate-density clouds will be shocked and ionized, cooling back via Lyman- α emission. These shocks may also re-accelerate any older, cooler relativistic electrons caught in the magnetic fields around the radio galaxy. In this picture, there is a direct physical correspondance between regions of Lyman- α emission, relativistic electrons and X-ray emission as the electrons cool via IC scattering off CMB and local FIR photons. The need for a more localized electron “re-heating” is also suggested by comparing the ~ 100 Myr crossing time of the 4C 41.17 system to the IC cooling time of the electrons (assuming CMB photons only): $2.1 \times 10^{12} / [\gamma(1+z)^4]$ yr (Schwartz 2002b), which is ~ 4 Myr for $\gamma = 1000$ at $z = 3.8$. Further support comes from the detection of high-velocity outflowing gas around 4C 41.17. Both the [OII] and Lyman- α emission lines exhibit large blue-shifted velocities (~ 600 – 900 km s $^{-1}$) along the direction of the principle radio axis and South-Western Lyman- α filament, together with Lyman- α velocity widths in this filament as high as ~ 900 – 1600 km s $^{-1}$ (van Breugel et al. 2002). Along this axis it seems likely therefore that shock heating of the gas will play a major role in powering the Lyman- α emission, and potentially contributing to the accelerated electron population responsible for the IC X-ray emission. Away from this axis however the situation is less clear, since there is still widely distributed IC X-ray emission with correlated and quite uniform, Lyman- α emission.

5. Feedback and galaxy growth

Finally, and most excitingly, it may be possible for the X-ray emission to produce Lyman- α emission through local photo-ionization of gas. The ionization parameter can be estimated to order of magnitude as: $\xi \sim (10^{45} \text{ergs}^{-1}) / nl^2$, where n is the mean gas density (cm $^{-3}$) and l is the physical scale of the gas distribution. Taking $l \sim 100$ kpc then $\xi \sim 1/n100$. We know that [O II] and [O III] species exist in the halo gas (van Breugel et al. 2002), consequently ξ must be in the range 1–10 (Kallman & McCray 1982), and probably towards the lower end in order for the recombination Lyman- α emission to be seen. Very crudely then, if the typical halo gas density is *less* than ~ 0.001 cm $^{-3}$ (as suggested from the rotation measure, Carilli, Owen, & Harris (1994)) the observed X-ray emission would photoionize the gas to much higher species than observed. However, in the denser regions it would appear that direct photoionization by the IC X-ray emission is another viable, if

not inescapable, mechanism for creating the ionized Lyman- α halo. This mechanism could operate either in addition to, or independently of the shock driven ionization, depending on the location relative to the principle jet/out-flow axis as discussed above. At the present moment it is impossible to differentiate between these scenarios, but future optical and near-IR IFU observations of the spatial distribution of a range of emission lines in the halo of 4C41.17 will be a powerful technique to investigate the internal physics of this galaxy.

If it can be demonstrated that it operates, this new IC X-ray photoionization mechanism presents the AGN within 4C41.17 with another route to exert feedback on the surrounding gas halo on a larger scale than could be directly surmised from the properties of the radio jets. Moreover, this feedback mechanism may continue to operate after the radio activity has ceased to be directly detectable. Combined with the mechanical energy input of the relativistic electrons, which is likely responsible for the X-ray cavities seen in low- z clusters (Fabian et al. 2003a), these represent two major pathways for supermassive black holes to exert significant feedback on scales extending beyond their host galaxies.

Perhaps the most important feature of this mechanism is that it is expected to be most effective in the most massive halos at the highest redshifts: those which have been able to build a supermassive black hole large enough to power powerful radio jets. The mass-specific nature and redshift dependency of this feedback mechanism may provide a new avenue for theoretical attempts to model the formation and growth of the most massive galaxies and clusters seen in the local Universe (Benson et al. 2003; Wu, Fabian, & Nulsen 2000).

6. Conclusion

We have detected extended X-ray emission around the luminous radio galaxy 4C41.17 at $z = 3.8$. The spectral properties of the diffuse X-ray emission are best described by a power-law model, with a spectral index which is consistent with that seen in the radio waveband. Moreover, the morphology of the X-ray emission correlates well with the general distribution of radio emission. We propose that Inverse Compton scattering is the mostly likely origin of the X-ray emission and we limit any contribution from thermal emission by hot gas to less than $4 \times 10^{43} \text{ erg s}^{-1}$.

We quantify our discussion of IC scattering around 4C41.17 and conclude that if the equipartition estimates of magnetic field strength are valid then the observed X-ray emission is due to the scattering of both CMB and local FIR photons. The detection of the galaxy as a very bright submm source supports this hypothesis. We compare two simple geometrical models for the thermal dust emission around 4C41.17. The X-ray requirements for the mean

FIR energy density in the plasma volume are that $\rho_{FIR} = 1 - 3 \times \rho_{CMB}$. The constraints that this imposes on the volume of the FIR emitting region are consistent with the crude, direct measurements of the size of the galaxy in the submm waveband, which imply that the dust emission is extended over ~ 50 kpc scales (although subject to considerable uncertainty).

We demonstrate that IC X-ray emission, enabled by the enhanced CMB at high redshift and the local FIR luminosity of this highly-obscured, active system, can readily ionize the gas in the halo of this galaxy. While it is unlikely that this is the sole mechanism by which the Lyman- α halo is produced, it seems inevitable that it plays a significant role, especially away from the large out-flow velocities seen along the principle radio axis. It could also be very efficient at ionizing the less dense, outer halo. Importantly, if the observed Lyman- α emission is recombination following photo-ionization then this gas could also have a significantly lower temperature, and shorter cooling time.

IC X-ray emission from high- z supernovae has been suggested as a reionization mechanism in the early universe (Oh 2001), with profound implications for the formation of stars and galaxies. On the basis of our results presented here we are compelled to add that IC X-ray emission from early AGN activity should also be an important feedback mechanism – especially given that the diffuse IC emission from the CMB can easily exceed that directly due to accretion onto the central black hole, and that its diffuse nature permeates the halo volume more thoroughly. Moreover, this form of feedback will operate preferentially in the most massive halos, those which are able to host powerful radio galaxies. This mechanism, together with the mechanical energy injected by the AGN via relativistic electrons may therefore address the fundamental problem of overcooling in models of the formation of massive galaxies and clusters in the local universe (Benson et al. 2003; Wu, Fabian, & Nulsen 2000). As we have shown, 4C 41.17 exhibits three of the main features currently expected to regulate star formation in massive galaxies (Benson et al. 2003): an ordered magnetic field (detected as a strong rotation measure) to allow conduction of heat from the outskirts of the halo into the centre and so suppress the cooling of gas; AGN-driven feedback in the form of the mechanical input from the radio jets and lobes; and outflows associated with visible and obscured massive star formation. However, it is intriguing that even this combination of three mechanisms apparently hasn't *yet* been able to suppress the star formation in this massive galaxy (Dey et al. 1997; Ivison et al. 2001).

Finally, we suggest that the combination of intense, but obscured, activity in 4C 41.17, coupled with its high redshift, and hence the strong increase in the energy density of the CMB, has aided in our identification of the X-ray halo around this galaxy. If correct this would imply that large halos, containing large populations of low energy electrons (tracers of past radio activity), ordered magnetic fields and significant quantities of ionized gas, may

be common around all massive galaxies at high redshifts, $z \geq 1$. If the IC X-ray emission plays an important photo-ionization role this would also provide an additional mechanism for switching on Lyman- α halos at high- z by radio activity and the CMB/FIR photons alone. Clearly the rapid decline in the energy density in the CMB, coupled with a similar strong decline in the typical FIR luminosities of active galaxies at $z < 2$ (Archibald et al. 2001; Page et al. 2001) mean that IC scattered X-ray halos should rapidly decrease in intensity at lower redshifts.

Together with existing data from other wavebands these *Chandra* results point towards an extraordinary environment in systems like 4C 41.17. The central AGN is periodically injecting high energy electrons and energy through the length of the medium in which it is embedded. This medium is truly multi-phase, consisting of $\sim 50\text{K}$ dust distributed over 10–20% of the 100–150 kpc wide system volume, co-existing with the largest Lyman- α halo known along with cooler dust, magnetic fields, intense UV flux from massive star formation, and flooded by X-ray photons.

As the construction site of a massive galaxy, and almost certainly what will become the core of a massive cluster of galaxies, this system directly illustrates the extent to which astrophysics helps mold the nature of the relatively quiet cluster environments we see today. The radio observations of 4C 41.17 suggest that it is surrounded by a large mass of gas, which would be a significant component in the ICM of any present-day cluster, although it has yet to be heated or compressed sufficiently at $z = 3.8$ to be visible in the X-ray waveband. The coincidence of this phase of growth with the wide range of energetic phenomenae we observe in 4C 41.17 suggest that these phenomenae may play a role in setting the final physical characteristics of the ICM – such as establishing a minimum entropy for gas in clusters at the present-day. Future X-ray observations of other high- z radio galaxies will lead to a more unified picture of energetics and feedback mechanisms in these systems.

We acknowledge Jason Stevens and Jim Dunlop for their work on the submm properties of 4C 41.17. We also acknowledge useful discussions with David Helfand and Frits Paerels. This work was made possible by the exceptional capabilities of the NASA/*Chandra* observatory, and the dedicated support of the CXC. C.A.S. acknowledges the support of NASA grant NAG5-6035, and NASA/*Chandra* grant SA0 G02-3167X, I.R.S. acknowledges support from the Royal Society and Leverhulme Trust. R.G.B. acknowledges support from PPARC and the Leverhulme Trust. The work by W.v.B. and M.R. was performed under the auspices of the U.S. Department of Energy by the University of California, Lawrence Livermore National Laboratory under contract No. W-7405-Eng-48. W.v.B. also acknowledges NASA grants GO 5940, 6608 and 8183 in support of high redshift radio galaxy research with HST. Finally, we thank the referee D. Harris for comments which have substantially improved this

manuscript.

REFERENCES

- Archibald, E. N., Dunlop, J. S., Hughes, D. H., Rawlings, S., Eales, S. A., Ivison, R. J., 2001, *MNRAS*, 323, 417
- Benson, A. J., Bower, R. G., Frenk, C. S., Lacey, C. G., Baugh, C. M., Cole, S., 2003, *ApJ* submitted, astro-ph/0302450
- Bicknell, G. V., Sutherland, R. S., van Breugel, W. J. M., Dopita, M. A., Dey, A., & Miley, G. K. 2000, *ApJ*, 540, 678
- Boehringer, H., Voges, W., Fabian, A. C., Edge, A. C., & Neumann, D. M. 1993, *MNRAS*, 264, L25
- Brunetti, G., Cappi, M., Setti, G., Feretti, L., & Harris, D. E. 2001, *A&A*, 372, 755
- Brunetti, G. 2002, astro-ph/0208074
- Carilli, C. L., Owen, F. N., & Harris, D. E. 1994, *AJ*, 107, 480
- Carilli, C. L., Perley, R. A., & Harris, D. E. 1994, *MNRAS*, 270, 173
- Carilli, C. L., Harris, D. E., Pentericci, L., Rottergering, H. J. A., Miley, G. K., & Bremer, M. N. 1998, *ApJ*, 494, L143
- Carilli, C. L., Harris, D. E., Pentericci, L., Röttgering, H. J. A., Miley, G. K., Kurk, J. D., & van Breugel, W. 2002, *ApJ*, 567, 781
- Celotti, A., Ghisellini, G., & Chiaberge, M. 2001, *MNRAS*, 321, L1
- Chambers, K. C., Miley, G. K., & van Breugel, W. J. M. 1990, *ApJ*, 363, 21
- Chapman, S.C., McCarthy, P.J., Persson, S.E., 2000, *AJ*, 120, 1612
- Chartas, G. et al. 2000, *ApJ*, 542, 655
- Chartas, G., & Getman, K. 2002, <http://www.astro.psu.edu/users/chartas/xcontdir/xcont.html>
- Cole, S., Lacey, C. G., Baugh, C. M., & Frenk, C. S. 2000, *MNRAS*, 319, 168
- Comastri, A., Brunetti, G., Dallacasa, D., Bondi, M., Pendani, M., & Setti, G. 2003, *MNRAS*, in press

- Crawford, C., Lehmann, I., Fabian, A.C., Bremer, M.N., Hasinger, G., 1999, MNRAS, 308, 1159
- Dey, A., van Breugel, W., Vacca, W. D., & Antonucci, R. 1997, ApJ, 490, 698
- Donahue, M., Daly, R.A., Horner, D.J., 2003, ApJ, in press
- Evrard, A. E. & Henry, J. P. 1991, ApJ, 383, 95
- Fabian, A. C., Crawford, C. S., Ettori, S., & Sanders, J. S. 2001, MNRAS, 322, L11
- Fabian, A. C., Sanders, J. S., Crawford, C. S., Ettori, S. 2003a, astro-ph/0301468
- Fabian, A. C., Celotti, A., & Johnstone, R. M. 2003b, MNRAS, 338, L7
- Felten, J. E. & Morrison, P. 1966, ApJ, 146, 686
- Fixsen, D. J., Cheng, E. S., Gales, J. M., Mather, J. C., Shafer, R. A., & Wright, E. L. 1996, ApJ, 473, 576
- Harris, D. E., & Krawczynski, H. 2002, ApJ, 547, 740
- Herbig, T. & Readhead, A. C. S. 1992, ApJS, 81, 83
- Iverson, R. J., Dunlop, J. S., Smail, I., Dey, A., Liu, M. C., & Graham, J. R. 2000, ApJ, 542, 27
- Jones, F. C., 1965, Phys. rev. B, 137, 1306
- Kaiser, N. 1991, ApJ, 383, 104
- Kallman, T. R. & McCray, R. 1982, ApJS, 50, 263
- Kurk, J.D., Röttgering, H.J.A., Pentericci, L., Miley, G.K., van Breugel, W., Carilli, C.L., Ford, H., Heckman, T., McCarthy, P., Moorwood, A., 2000, A&A, 358, L1.
- Lacy, M. & Rawlings, S. 1996, MNRAS, 280, 888
- McNamara, B. R. et al. 2000, ApJ, 534, L135
- Mushotzky, R. F. & Scharf, C. A. 1997, ApJ, 482, L13
- Oh, S. P. 2001, ApJ, 553, 499
- Page, M. J., Stevens, J. A., Mittaz, J. P. D., Carrera, F. J., 2001, Science, 294, 2516

- Pentericci, L., Kurk, J.D., Carilli, C.L., Harris, D.E., Miley, G.K., Röttgering, H.J.A., 2002, *A&A*, 369, 109
- Pentericci, L., Kurk, J.D., Röttgering, H.J.A., Miley, G.K., van Breugel, W., Carilli, C.L., Ford, H., Heckman, T., McCarthy, P., Moorwood, A., 2000, *A&A*, 361, L25.
- Rees, M. J. 1989, *MNRAS*, 239, 1P
- M. Reuland, W. van Breugel, H. Röttgering, d. W., S. Stanford, A. Dey, M. Lacy, J. Bland-Hawthorn, M. Dopita, and M. Miley 2003, *ApJ*accepted, astro-ph/0303637
- Rosati, P. et al. 2002, *ApJ*, 566, 667
- Schwartz, D. A. et al. 2000, *ApJ*, 540, L69
- Schwartz, D. A. 2002a, *ApJ*, 569, L23
- Schwartz, D. A. 2002b, *ApJ*, 571, L71
- Sheinis, A. I., Miller, J. S., Bolte, M., & Sutin, B. M. 2000, *Proc. SPIE*, 4008, 522
- Siemiginowska, A., Bechtold, J., Aldcroft, T. L., Elvis, M., Harris, D. E., & Dobrzycki, A. 2002, *ApJ*, 570, 543
- Smail, I., Ivison, R. J., Blain, A. W., & Kneib, J.-P. 2002, *MNRAS*, 331, 495
- Spergel, D. N. et al. 2003, astro-ph/0302209
- Steidel, C. C., Adelberger, K. L., Giavalisco, M., Dickinson, M., & Pettini, M. 1999, *ApJ*, 519, 1
- Stevens, J. A., Ivison, R. J., Dunlop, J. S., Smail, I., Hughes, D. W., Röttgering, H. J. A., van Breugel, W. J. M., Reuland, M. 2003, *Nature*, submitted
- Tozzi, P. & Norman, C. 2001a, *ApJ*, 546, 63
- Tozzi, P. et al. 2001b, *ApJ*, 562, 42
- van Breugel, W., Stanford, A., Dey, A., Miley, G., Stern, D., Spinrad, H., Graham, J. and McCarthy, P., Induced star formation and morphological evolution in very high redshift radio galaxies, *KNAW Proc. ‘The Most Distant Radio Galaxies’*, Amsterdam 1999, Vol. 49, pg 49 (and 311, 312 for color pictures)
- van Breugel, W. et al. 2002, astro-ph/0209173

Voit, G. M., Bryan, G. L., Balogh, M. L., & Bower, R. G. 2002, ApJ, 576, 601

Worrall, D.M., Birkinshaw, M., Hardcastle, M.J., Lawrence, C.R., 2001, MNRAS, 326, 1127.

Wu, K. K. S., Fabian, A. C., & Nulsen, P. E. J. 2000, MNRAS, 318, 889

Fig. 1.— $25'' \times 25''$ image of 4C 41.17 in the 0.3-5 keV band, smoothed using a Gaussian of width $0.5''$ to illustrate the strong, unresolved nuclear point source and extended low-surface brightness emission on a scale of $15''$ or 100 kpc (image credit H. Jessop). North is up, East to the left.

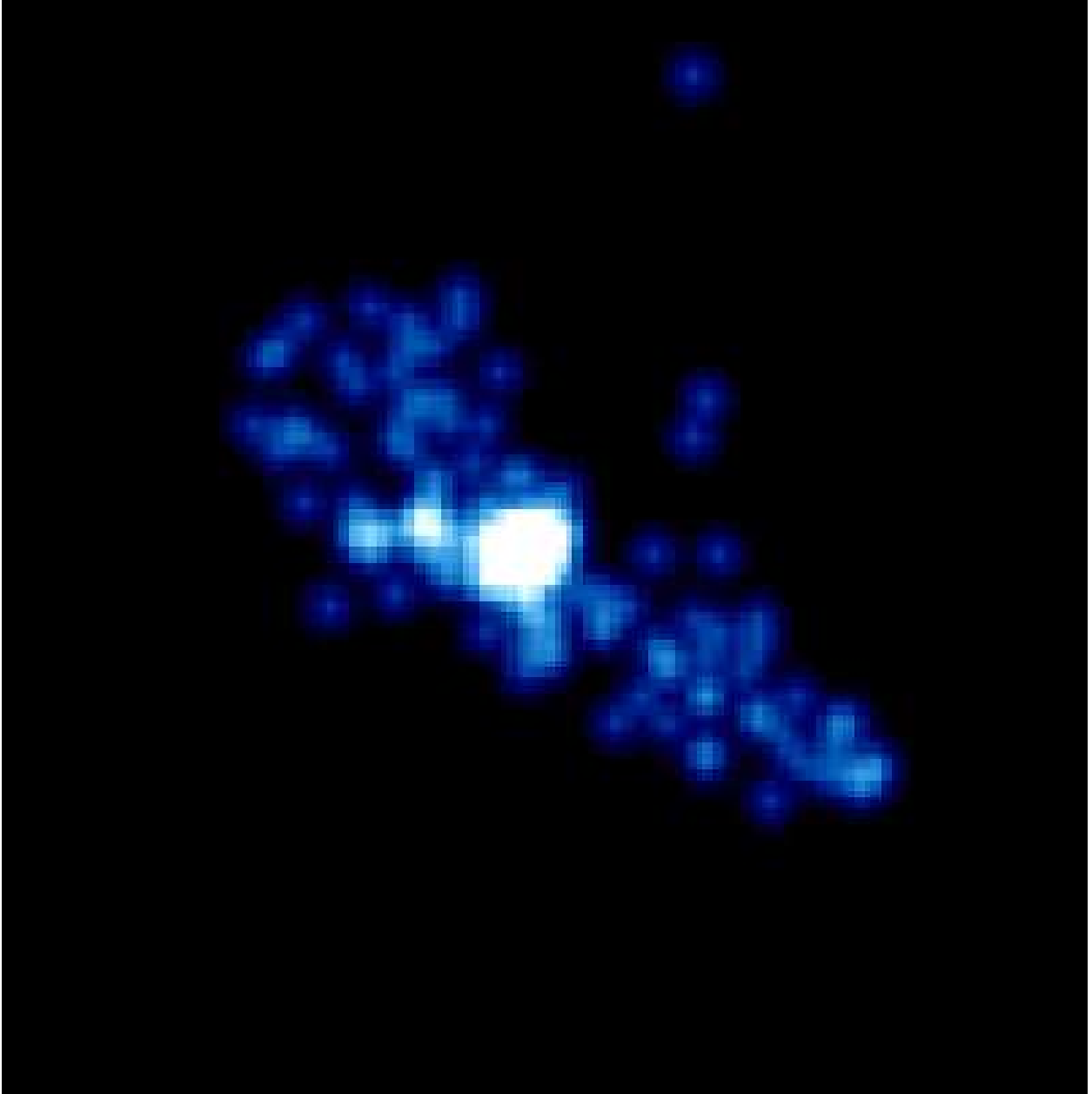


Fig. 2.— Three comparisons of 4C 41.17 in different wavebands. All three panels show a $20'' \times 20''$ field with North top and East to the left. The left-hand panel shows a true color *Chandra* X-ray image of the source coded as 0.2–1.5 keV (red), 1.5–2.5 keV (green) and 2.5–8.0 keV (blue), with the $850\mu\text{m}$ SCUBA map overlaid (Iverson et al. 2000). The lowermost submm contour is at 2.6 mJy per beam, subsequent contours are at 2.9, 3.4, 4.1, and 5.3 mJy per beam, to best illustrate the morphology. The submillimeter source is marginally resolved by the $15''$ FWHM SCUBA beam (Stevens et al. 2003). The central panel is the *Chandra* 0.5–2.0 keV soft-band image smoothed to match the beam-size of the overlaid 1.4 GHz VLA map. The X-ray gray-scale runs from 0.08–0.8 counts per $0.5''$ pixel, the 1.4GHz contours are at 0.3, 1.9, 10.9, 21.2, 37.5, 63.3 and 104.2 mJy per pixel. The rightmost panel shows the 2–10 keV hard-band image in grayscale (0.08–0.8 ct per $0.5''$ pixel) overlaid with the 4.9GHz contours (0.08, 0.5, 1.1, 2.2, 3.8 mJy per pixel). We label on this figure the various radio components using the naming scheme from Chambers, Miley, & van Breugel (1990). Although correlated, the outermost radio peaks do not coincide with the major components of the rather flat X-ray emission – consistent with an origin in different electron populations (§3) and with a contribution from a spatially uniform photon source population such as the CMB.

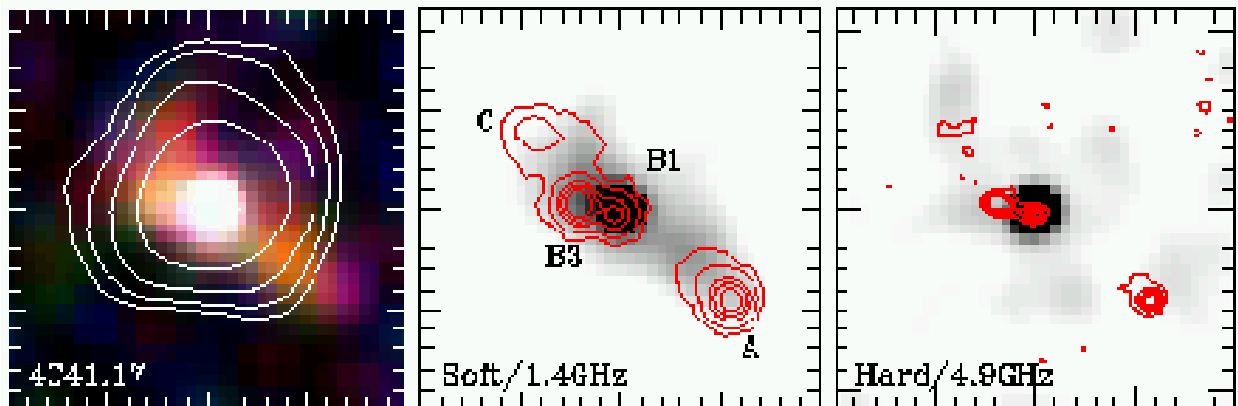


Fig. 3.— Left panel is $20'' \times 20''$ region showing adaptively smoothed 0.5–2 keV *Chandra* data (lowermost contour 0.05 ct per $0.5''$ pixel, linear increments of 0.1 ct per pixel) overlaid on 1.4GHz radio map grayscale (logarithmic intensity scaling, 0.01 – 2 mJy). Right panel is $40'' \times 40''$ region showing 0.5–2 keV X-ray data binned to $1''$ pixels (grayscale 0–6 cts per pixel) commensurate with the on-axis *Chandra* PSF. The region used to extract counts for the diffuse emission is shown as an ellipse in the right panel.

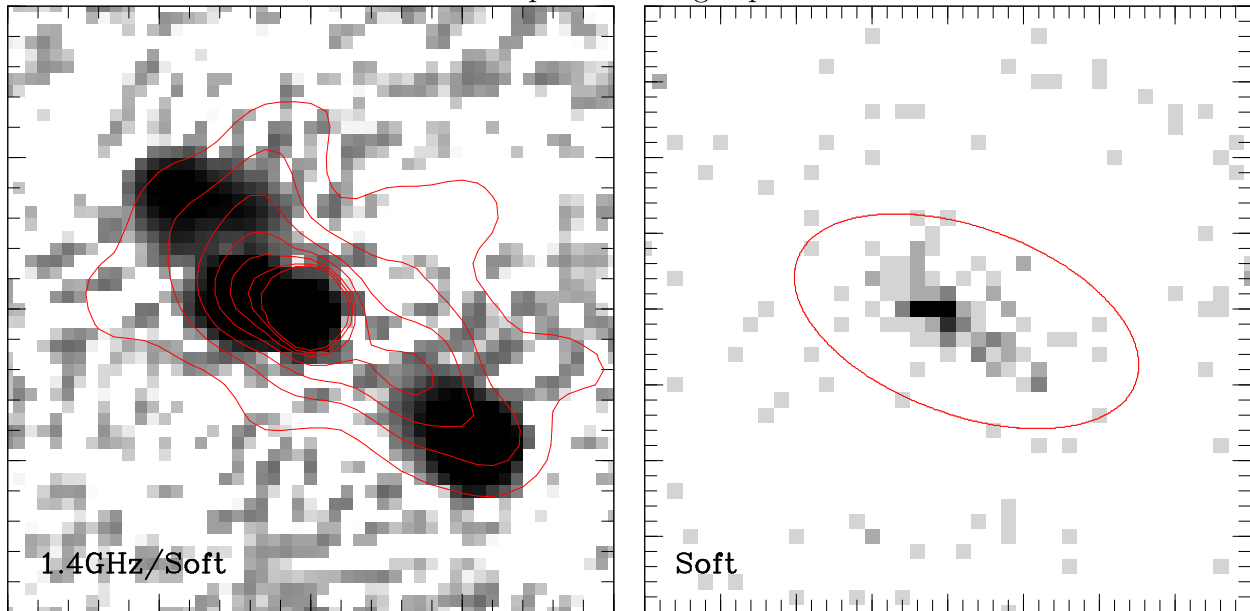


Fig. 4.— The binned spectrum of diffuse emission from 4C 41.17 across the energy range 0.3–10 keV (1.4–48 keV in the restframe), with the best fit model plotted as a solid curve and the residuals shown in the bottom panel. We conclude that this spectrum is well-fit (reduced $\chi^2 = 1.3$) by a single slope power law with an index of 1.29 ± 0.18 (90% confidence limits) and $n(\text{HI})$ fixed at the Galactic value of $1 \times 10^{21} \text{ cm}^{-2}$. A comparison of the fits for the extended X-ray emission to the North-east and South-west of the point source shows no significant difference in the spectral properties of these two regions.

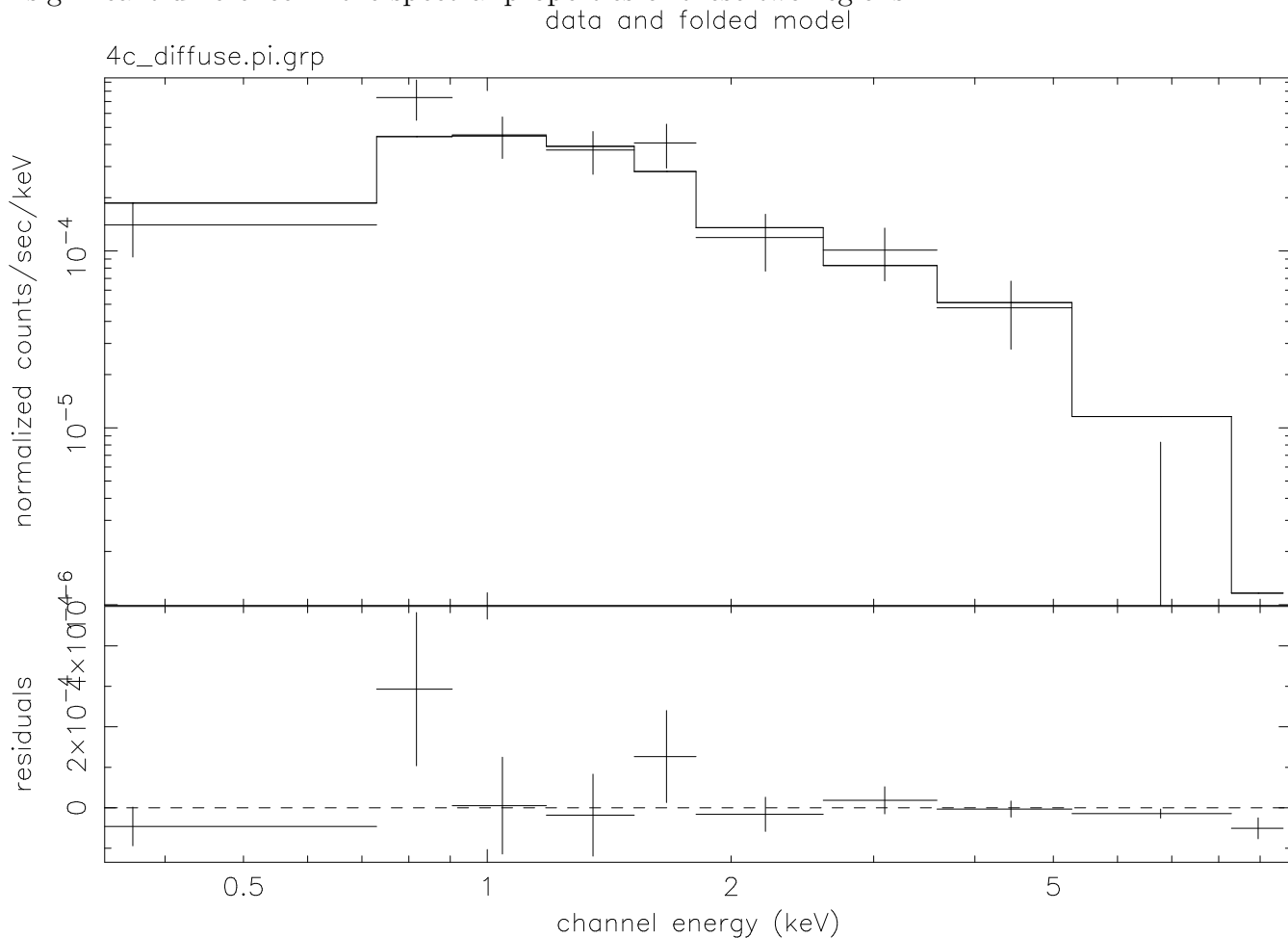


Fig. 5.— The predicted IC X-ray luminosity in the 1.44-48 keV rest frame (0.3-10 keV observed) is plotted versus the magnetic field strength in the relativistic electron population. The lowermost, light curve is the prediction for scattering from CMB photons only (energy density ρ_{CMB}). Curves of increasing L_x correspond to the addition of a local FIR photon mean energy density in multiples of the CMB energy density: lowest curve $\rho_{FIR} = \rho_{CMB}$, middle $\rho_{FIR} = 2\rho_{CMB}$, uppermost $\rho_{FIR} = 3\rho_{CMB}$. Vertical lines indicate the range of estimated equipartition magnetic field strength (Carilli, Owen, & Harris 1994). Horizontal dashed lines indicate the allowed range of *observed* X-ray luminosity in the 4C41.17 diffuse emission.

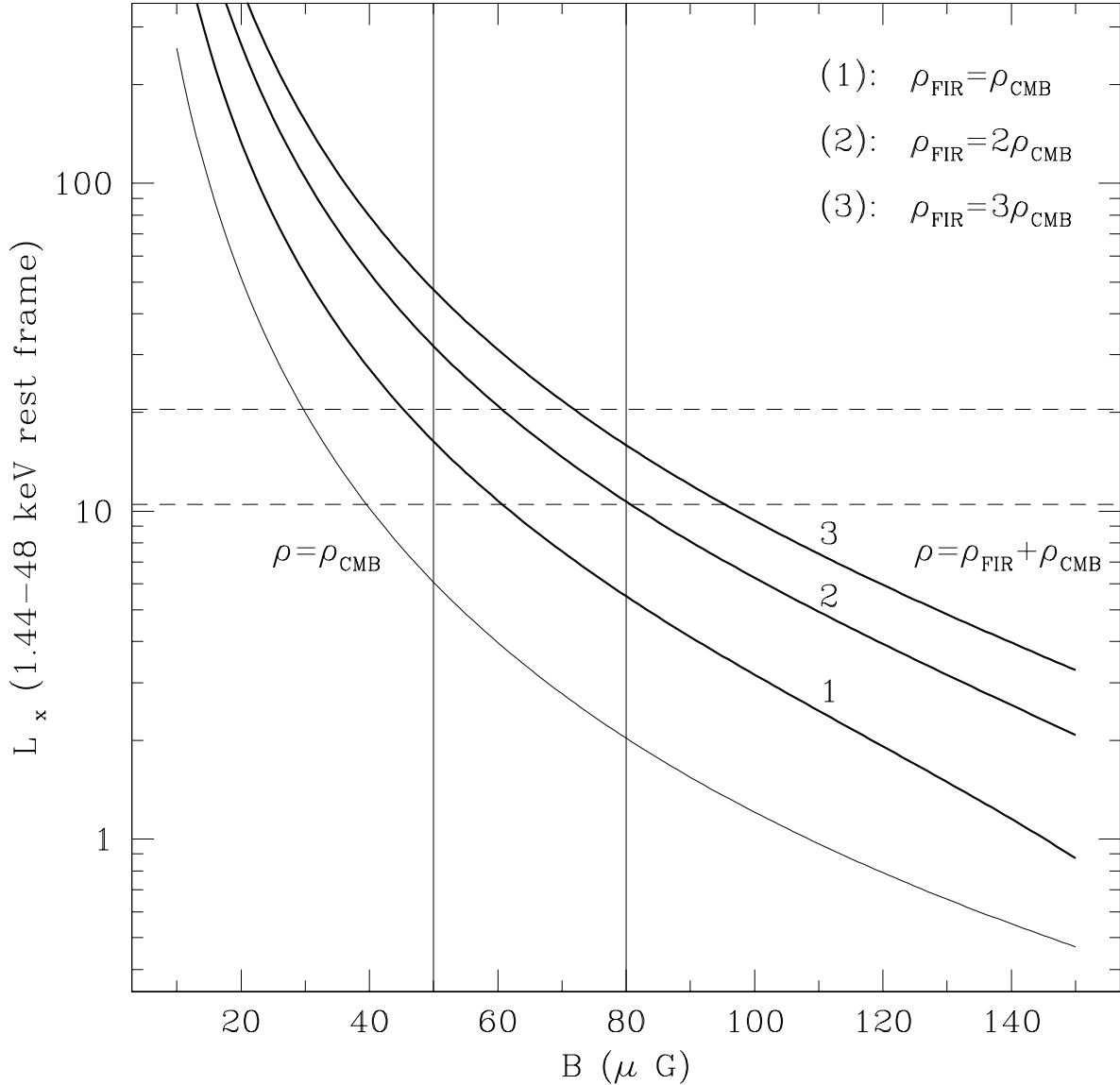


Fig. 6.— (a) The left-hand panel shows the high surface brightness regions of the Lyman- α emission (Reuland et al. 2003) around 4C 41.17 overlaid as contours (lowermost 0.22 ct per 0.21'' pixel, linear increments of 0.3 ct per pixel) on the *HST* WFPC2 F702W image of the galaxy (Ivison et al. 2000); (b) the central panel shows the 0.3–10 keV adaptively smoothed *Chandra* data as red contours (lowermost 0.18 ct per 0.5'' pixel, linear increments of 0.15 ct per pixel) overlaid on the Lyman- α image of 4C 41.17 (grayscale 0.01-2 ct per 0.21'' pixel), the brightest regions of which are also denoted by contours (lowermost 0.4 ct per pixel, increment 0.4 ct per pixel); (c) the right-hand panel shows the 1.4 GHz radio map as contours (red, levels 0.3, 1.9, 10.9, 21.2, 37.5, 63.3, 104.2 mJy per pixel) overlaid on the Lyman- α image (as in b)). All panels are 20'' \times 20'' (142 kpc at $z = 3.8$) and have North top and East to the left. We draw particular attention to the apparent correlation between structures in the Lyman- α and X-ray wavebands shown in the central panel. For example, the Northern arm of the crescent-like Lyman- α feature at [2'', -2''] (relative to the center of the galaxy) appears correlated with a ridge in the X-ray emission, and to some extent with the 1.4 GHz radio emission. Similarly, in the North/North-West of the halo three spur-like Lyman- α features are seen, with matching features in the outermost X-ray emission. These X-ray features are also evident in the both the soft (0.5–2 keV, 2.4–9.6 keV rest frame) and hard (2–10 keV, 9.6–48 keV rest frame) bands in Figure 1.

